J Polym Environ (2017) 25:1198–1207
DOI 10.1007/s10924-016-0897-x

ORIGINAL PAPER

Influence of Organically Modified Nanoclay on Thermal and Combustion Properties of Bagasse Reinforced HDPE Nanocomposites

Behzad Kord[1] · Pouria Ravanfar[2] · Nadir Ayrilmis[3]

Published online: 23 November 2016

Abstract The nanocomposites of high density polyethylene (HDPE)/bagasse flour (BF) with different contents of the organomodified montmorillonite (OMMT) were produced by melt blending process. The thermal stability and combustion behavior of nanocomposites were characterized by thermogravimetric analysis (TGA), differential scanning calorimetry, and cone calorimeter tests. The results of TGA data of the nanocomposites indicated that the OMMT greatly enhanced the thermal stability, and char residues of the HDPE/BF blends gradually increased with increasing the OMMT content. The activation energy was determined to describe the energy consumption of the initiation of the thermal degradation process. The composites produced with the 6 phc OMMT had the highest activation energy values among the evaluated composites (106 kJ/mol), whereas composites without nanoclay exhibited the lowest one. Furthermore, as the OMMT was incorporated into the nanocomposites, the melting temperature (T_m), crystallization temperature (T_c) melting enthalpy (ΔH_m) and crystallinity (X_c) of HDPE/BF blends increased. The findings showed that the OMMT effectively boosted the flame retardancy of nanocomposites due to the formation of the carbonaceous silicate char shields delayed time to ignition and the combustion process was remarkably hindered.

Keywords Nanocomposites · Organomodified montmorillonite · Thermal stability · Flame retardancy

✉ Behzad Kord
b.kord@standard.ac.ir

Nadir Ayrilmis
nadiray@istanbul.edu.tr

[1] Department of Paper and Packaging Technology, Faculty of Chemistry and Petrochemical Engineering, Standard Research Institute (SRI), P.O. Box 31745-139, Karaj, Iran

[2] Department of Wood and Paper Science and Technology, Chalous Branch, Islamic Azad University, Chalous, Iran

[3] Department of Wood Mechanics and Technology, Forestry Faculty, Istanbul University, 34473 Bahcekoy, Sariyer, Istanbul, Turkey

Introduction

During the last few decades, thermoplastics have gained ever-increasing acceptance as an important family of engineering materials and are steadily replacing metals in a wide variety of applications. The commercial consumption of thermoplastics has steadily increased, and this trend is expected to continue despite an increase in their prices. This situation has created an impetus for cost reduction via composites by employing fillers in thermoplastics [1]. In the recent years, organic reinforcements such as natural fibers have penetrated slowly into the market of thermoplastic composites. This was because the natural fibers they offer many advantages over most common inorganic fillers such as a reduced wear of processing equipment and are renewable, recyclable, non-hazardous, and biodegradable. Natural fibers are abundantly available and have lower costs and density. The replacement of inorganic fillers with comparable natural fibers provides weight savings and decreases the cost of materials without reducing the rigidity of the composites [2, 3].

Wood plastic composites (WPCs) are defined as composite materials containing wood (in various forms such as flour or fiber) and polymer materials. These materials are a relatively new family of composite materials, in which a natural fiber (such as wood flour/fiber, kenaf fiber, hemp,

sisal, etc.) is mixed with a commodity thermoplastic such as polyethylene (PE), polypropylene (PP), poly(vinyl chloride) (PVC), etc. WPCs are becoming more and more commonplace by the development of new production techniques and processing equipment. Around 100 companies involved in WPC manufacturing have been identified worldwide [1–3].

Natural fibers have several advantages, such as being inexpensive, being renewable, being lower density, undergoing little damage during processing, and their disposal causing minor ecological impact. However, there are disadvantages as well. Such as incompatibility between the hydrophilic natural fibers and the hydrophobic plastic part, low bulk density and in turn, agglomeration and difficulty in processing, water absorption and lower dimensional stability and the last but not least thermal instability of natural fibers during processing at high temperatures [4, 5].

Low thermal stability of most natural fibers is an obstacle in the production of thermoplastic composites. In order to avoid degradation of the natural fibers, the processing temperature is kept below the degradation temperature of the natural fibers (usually below 200 °C). The degradation of the natural fibers can lead to brittleness and poor mechanical integrity of thermoplastic composites [6]. Thermal degradation is also an important aspect in the development of natural fibers composites since it will strongly affect the maximum temperature used in the processing of the composites and will indirectly determine the maximum retention time of the materials in the processing system. Thermal degradation is therefore, one major limitation frequently encountered when using natural fibers as reinforcement in a polymeric matrix [5, 6]. The most common technique to investigate the mass change, thermal decomposition, and thermal stability of composite materials is thermal gravimetric analysis (TGA) [4]. In addition, knowledge of the kinetic parameters associated with thermal degradation constitutes an important tool in estimating the thermal behavior of such composites [4–6].

Polymer nanocomposites based on layered nanoclays have attracted a great deal of interest because they exhibit remarkable improvement of mechanical, thermal, and barrier properties when compared with those of pure polymer or conventional composites [7]. Smectic clays, particularly montmorillonite (MMT) minerals, serve as good nanoclay fillers owing to their ease of dispersability in the organic matrix. MMT is composed of aluminum silicate layers, which are organized in a parallel fashion to form stacks with a regular Van der Waals gap in between them called interlayer spacing or gallery [7–9]. Clays are in nature organophobic, but they can be chemically changed into organophilic by replacing the Na^+, K^+, Ca^{+2} or Mg^{+2} cation originally present in the galleries with one organic cation such as alkylammonium ions via an ion-exchange reaction [8]. Besides this, MMT is naturally occurring, environment friendly, cheap, and readily available in large quantities [9]. Nowadays, the application of organo-modified montmorillonite (OMMT) as a nano-sized reinforcement in WPCs has been developed. It is evident that the addition of small amount of nanoclay (3–5 wt%) substantially enhance the WPCs performance [10–22].

In this research work, the morphological, mechanical, thermal, and combustion characteristics of HDPE/bagasse composites filled with organically modified nanoclay were extensively investigated.

Experimental

Materials

High density polyethylene (HDPE), with trade name of HD5620EA, an injection molding grade was supplied by Arak Petrochemical Co. (Iran). The HDPE was in the form of pellets with a melt flow index of 20 g/10 min and density of 0.95 g/cm^3. Mechanical properties of neat HDPE were as follows: tensile strength 22 MPa, tensile modulus 900 MPa, elongation at break 700%, flexural modulus 1000 MPa, and impact strength 30 kJ/m^2. Polyethylene-grafted maleic anhydride (PE-g-MA) was obtained from Eastman Chemical Co. (Kingsport, TN, USA). Epolene G-2608 has a melt flow index of 6–10 g/10 min, an acid number of mg KOH/g, and weight average of $M_W \approx 65{,}000$ g/mol, as reported by the supplier. The organomodified montmorillonite (OMMT), with trade name of Cloisite 30B, in powder form was used as nanoclay. Natural montmorillonite modified with a bis-2-hydroxyethyl tallow quaternary ammonium (CEC = 90 meq/100 g clay, $d_{001} = 18.5$ Å) was obtained from Southern Clay Products Co. (Gonzalez, Texas, USA). Bagasse stalks were supplied by Khuzestan Cultivation and Industry Co., Iran. The bagasse stalks were depithed and cut to 2–3 cm in length by hand. They were then washed, air-dried, and screened through a series of screens to remove dirt. In order to reduce extractives effects, woody materials were treated with water at 50 °C for 48 h. The depithed bagasse stalks were ground with a Thomas–Wiley miller to fine powder of 60-meshsize, and then oven-dried and stored in sealed plastic bags before processing.

Method

Composite Preparation

Polyethylene, bagasse flour (BF) and nanoclay were weighed and bagged according to formulations given in Table 1. For all samples, the coupling agent was kept

Table 1 Compositions of the studied formulations

Sample code	HDPE (Wt%)	BF (Wt%)	OMMT (phc*)	PE-g-MA (phc)
A1	50	50	0	2
A2	50	50	2	2
A3	50	50	4	2
A4	50	50	6	2

HDPE high density polyethylene; *BF* bagasse flour; *OMMT* organomodified montmorillonite; *phc* parts by weight per hundred parts of compounds

constant at 2 phc (parts by weight per hundred parts of compounds) for all formulations. They were then blended at 180 °C for 13 min at 60 rpm using a Hake internal mixer (SYS 9000, USA). First, the HDPE granulates were fed to the mixing chamber. After HDPE melting, PE-g-MA and OMMT were added. RSF was fed at the 7th min, and the total mixing time was 13 min. The compounded materials were ground by using a pilot scale grinder (WIESER, WGLS 200/200 Model). The resulting granules were dried at 105 °C for 4 h. Test specimens were prepared by injection molding at 190 °C and 10 MPa (Eman machine, Iran). The specimens were stored under controlled conditions (50% relative humidity and 23 °C) for at least 40 h prior to testing.

Thermal Analysis

Thermogravimetric analysis (TGA) was used to investigate thermal decomposition behavior of samples with a Perkin Elmer 7 series apparatus thermogravimetric analyzer (TGA-Pyris 6 (Perkin Elmer instruments, England). Tests were done under high quality nitrogen (99.5% nitrogen, 0.5% oxygen content) atmosphere with a flow rate of 20 mL/min at a scan rate of 10 °C/min in a programmed temperature range of 25–600 °C. A sample of 10 mg was used for each run. Aluminum oxide was used as the reference material. At least three replications for each formulation were made and average curves were calculated. The weight change was recorded as a function of heating temperature. The rate of mass loss versus temperature was determined using derivative thermogravimetric (DTG) curve and software accompanying the analyzer.

The activation energy was determined to describe the energy consumption of the initiation of the thermal degradation process. The analysis of the activation energy was carried out based on the Broido equation and adjusting the experimental values to the following equation [17].

$$\ln\left(\frac{\ln 1}{y}\right) = \frac{-E_a}{RT} + \ln\left(\frac{RZ}{BT_{\max}^2}\right) \quad (1)$$

where y is the fraction of non-volatilized material not decomposed, T_{max} is the temperature of maximum reaction rate, β is the heating rate, Z is the frequency factor, and E_a is the activation energy. The activation energy was obtained from the slopes of the plots of $\ln\left(\frac{\ln 1}{y}\right)$ versus $\frac{1}{T}$ for various stages of thermal decomposition.

Differential scanning calorimetry (DSC) analyses were carried out under a nitrogen flow (20 ml min^{-1}) using a Netzsch (200F3 Maia, Germany). The sample weights were in the range of 5–10 mg, and they were heated from 25 to 300 °C at a heating rate of 10 °C min^{-1}. The same conditions were maintained for heating and cooling cycles. Three replicates were run for each specimen. For all the samples, the onset and peak temperatures of melting (T_m) and crystallization (T_c), as well as the melting enthalpy (ΔH_m) were determined from the second scan. The degree of crystallinity (X_c) was calculated as follows:

$$X_c = \frac{\Delta H_m}{\Delta H_m^\circ \times W} \times 100 \quad (2)$$

where ΔH_m is the enthalpy of the sample, ΔH_m^o is the enthalpy of a 100% crystalline HDPE taken as 292 J/g [4] and w is the mass fraction of HDPE in composites.

Combustion Properties

The combustion parameters such as heat release rate (HRR), time to ignition (TTI), mass loss rate (MLR), and burning rate (BR) can be obtained from cone calorimeter. The cone calorimeter test (Cone 2, Atlas) was carried out according to ASTM E1354 standard procedures. Each specimen with dimensions of 100 mm × 100 mm × 3 mm, was placed on an aluminum foil and exposed horizontally to an external heat flux of 5 kW/m^2. Limiting oxygen index (LOI) is defined as the minimum concentration of oxygen, expressed as percent volume, in a flowing mixture of oxygen and nitrogen that will support flaming combustion of a material initially at room temperature. According to this test, the higher the oxygen index, the lower flammable is the sample. The LOI technique was performed according to ASTM D2863 standard within 3 min.

Mechanical Testing

The flexural tests were conducted in accordance with ASTM D 790 using an Instron universal testing machine (model 4486, England) at a rate of 5 mm/min crosshead

speed. Dimensions of the test specimens were 100 × 13 × 5 mm^3. The tensile tests were measured according ASTM D790 specification on an Instron (model 4486). The specimens were tested at crosshead rate of 2 mm/min at room temperature. Dimensions of the test specimens (dogbone shape) were 167 × 10 × 3 mm^3. Five specimens were tested for the tensile and flexural properties of each composite formulation.

X-ray Diffraction

An X-ray diffractometer was used to measure the basal spacing between silicate layers in the nanocomposites. The XRD was performed in an X-ray diffractometer (Seifert-3003 PTS, Germany) using CuKα radiation ($\lambda = 1.54$ nm). The samples were scanned in 2θ ranges 2–10° at a rate of 1°/min. The generator was operated at 50 kV and 50 mA. The interlayer spacing (d_{001}) of clay was calculated in accordance with Bragg's law:

$$d = \frac{n\lambda}{2\sin\theta} \quad (3)$$

where d is the spacing between planes, θ is half of the angle of diffraction, n is the order of diffraction (n = 1), and λ is the X-ray wavelength of X-ray ($\lambda = 1.54$ nm).

Morphological Study

Studies on the morphology of the composites were carried out using a scanning electron microscope (SEM, WEGA-II TESCAN). The specimen was coated with a thin film (25 nm) of gold to avoid electrical charge accumulation during the examination and then analyzed at an accelerating voltage of 20 kV.

Result and Discussion

Thermal Behavior

TGA Analysis

The result of TGA test is illustrated in Fig. 1 which shows the residue weight of samples at different temperatures. It was found that all the samples had two main decomposition peaks. The first decomposition peak represents the degradation of the bagasse at temperatures around 320 °C (close to the main degradation of cellulose) and the second peak representing polyethylene degradation around 430 °C. According to the TGA curves, the degradation of baggase started at 240 °C, which was related to the low-temperature stage from degradation of cellulose and hemicelluloses and the high-temperature stage from degradation of lignin. The temperature of thermal degradation of hemicelluloses, cellulose, and lignin are between 150–350, 275–350, and 250–500 °C, respectively [4–6]. Therefore, the major sources of the first thermal degradation step in composites are the degradation of hemicelluloses, cellulose, and lignin [23, 24]. The mass loss from 40 to 130 °C (onset temperature for thermal decomposition) was related to the evaporation of water.

Furthermore, it was observed that the addition of nanoclay to the HDPE/BF blends increased the thermal stability of the composites. It was found that the addition of clay slightly improved the onset of the degradation of the composites. The increase of thermal stability was attributed to the hindered diffusion of volatile decomposition products by the clay particles in the polymer matrix [25–27]. The most likely explanation is that the well dispersed individual layers of intercalated/exfoliated clay platelets form torturous path, which inhibit the passage of volatile degradation product from the polymer matrix [28]. Moreover, strong interaction between nanoclay particles and HDPE chains could restrict chain movements and consequently retard conveying free radicals produced during fragmentation process of polymer as a result of thermal degradation [29, 30].

The corresponding TGA data including temperatures at the degradations of 10% (T_{10}), 25% (T_{25}), and 50% (T_{50}) degradation occurred and the residue at 600 °C was summarized in Table 2. Clearly, the degradation temperature shifted toward high temperature as the amount of nanoclay increased in the composite. As a result, the composites containing 6 phc OMMT had the highest the thermal stability in comparison with other nanocomposites. The nanometer level dispersed silicate layers interact strongly with the polymer chains and simultaneously, the barrier effect of silicate layers inhibit the mobility of small molecules produced as a result of thermal degradation. These two effects of silicate layers altogether contribute toward the enhancement of the thermal stability of the nanocomposites [28, 29].

The phenomena leading to the weight loss due to thermal degradation can be better studied using the derivative weight loss curves (DTG) which show the rate at which the materials decompose. These curves are presented in Fig. 2 for all the formulations. The thermal degradation of the HDPE/BF blends occurred in a two-step degradation process, which was confirmed by the presence of two peaks in the DTG curves. The first thermal degradation step was related to the hemicelluloses, cellulose, and lignin constituents in bagasse, and the second one to thermal degradation of HDPE. For the composite formulations, a small peak was observed at around 130 °C. This was due to the release of moisture of the samples. The samples used in the TGA tests were cut from the injection molded specimens

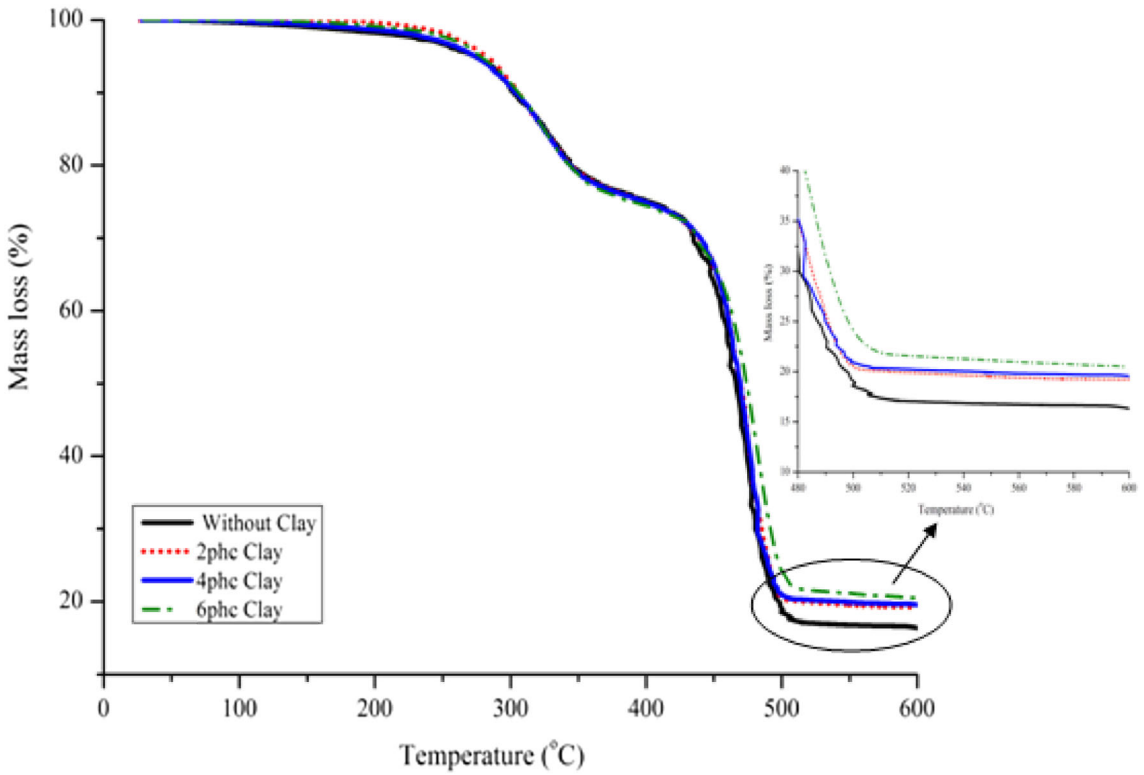

Fig. 1 TGA thermograms of HDPE/RF composites with different OMMT content

which lost moisture upon melting at a higher rate. The low temperature decomposition (left shoulder of DTG curve) occurred in the temperature range of 250–300 °C, which could be attributed to the thermal degradation of hemicelluloses which were the least thermally stable lignocellulosic component and the decomposition of HDPE. The second decomposition process was observed in the temperature range of 300–400 °C. It was believed that this region was related to the decomposition of cellulose [4–6, 23, 24]. The DTG curve analysis showed that the samples with addition of nanoclay experienced two-step processes; however, the latter had a higher decomposition temperature compared with the samples without nanoclay. The possible reason is that the amount of char residues that can be formed on the surface during combustion improved the thermal stability [25–30].

The larger is the activation energy, the greater is the thermal stability [24]. It could be seen from Table 3 that addition of nanoclay increased the activation energy. This

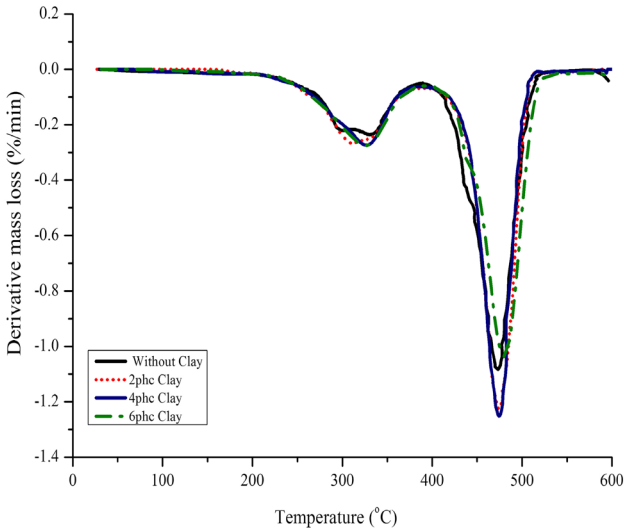

Fig. 2 DTG curves of HDPE/RF composites with different OMMT content

Table 2 Thermal properties of HDPE/RF composites with different OMMT content

Sample code	T10 (°C)	T25 (°C)	T50 (°C)	Char yield (%)
A1	295.4 ± 9.67	377.7 ± 6.33	460.8 ± 14.28	16.29 ± 0.27
A2	296.8 ± 12.42	378.5 ± 8.12	463.2 ± 13.61	19.13 ± 0.18
A3	297.3 ± 10.53	380.3 ± 5.79	467.4 ± 11.15	20.47 ± 0.33
A4	298.2 ± 11.08	381.1 ± 6.40	470.3 ± 12.43	21.64 ± 0.45

Table 3 Activation energies of HDPE/RF composites produced with different OMMT content

Sample code	Stages	Temperature range (°C)	Activation energy (kJ/mol)
A1	1st	305–360	67
	2nd	395–475	93
A2	1st	305–365	71
	2nd	390–480	98
A3	1st	305–370	75
	2nd	385–485	101
A4	1st	305–375	78
	2nd	380–490	106

indicated that the layered silicates serve as a thermal barrier in delaying the degradation process of HDPE in the nanocomposites [28]. The highest activation energy value was observed for the samples produced with 6 phc nanoclay, while the lowest one was recorded for the samples without nanoclay. The samples produced with 6 phc nanoclay increased activation energy from 67 to 78 and 93 to 106 kJ/mol for the first and second decomposition stages, respectively.

DSC Analysis

The thermal properties of the nanocomposite samples were also determined from DSC thermograms. The melting temperature (T_m), melting enthalpy (ΔH_m), crystallization temperature (T_c), and degree of crystallinity (X_c) of all the samples are listed in Table 4. The melting temperature increased towards higher temperatures with increasing nanoclay loading in the composites. It can be ascribed to the strong interaction between polymer matrix molecules and the layers of organoclay resulted in the immobilization of some polymer matrix as organoclay easily absorbed the polymer molecules. These freezed molecules of polymers are responsible for the crystallization process of nanocomposite. Therefore, the crystallization of polymer matrix molecules occurred at higher temperature, and the T_m values of nanocomposite systems are increased [22]. Furthermore, the T_c and degree of crystallinity (X_c) of composites without nanoclay (A_1) were found to be 114.5 °C and 34.89%, respectively. The introduction of fillers (clay and fiber) leads to an increase of crystallization temperature for HDPE. Lower crystallinity temperature indicates higher thermal stability because in composites, the fillers (clay or fibers) can absorb more energy than the polymer [21, 31].

The incorporation of 6 phc clay loading into the HDPE matrix resulted in an increase in the T_c to about 118.1 °C, with a degree of crystallinity (X_c) of 37.02%, which was due to heterogeneous nucleation of the nanoclays. The polymer molecular chains can crystallize by themselves through a self-nucleation effect (homogeneous nucleation) or by introducing a nucleating agent (heterogeneous nucleation) [21]. The nucleation effect is effective at low concentration (2 phc), but at higher content (6 phc) the high amount of fillers cannot effectively induce nucleation due to fillers–fillers contacts (agglomeration) and limited space for crystal nucleation/growth.

Table 4 Thermal parameters for the studied formulations determined from DSC

Sample code	T_m (°C)	T_c (°C)	X_c (%)
A1	134.3 ± 8.11	114.5 ± 5.33	34.89 ± 1.26
A2	136.7 ± 6.72	115.8 ± 4.65	35.99 ± 0.85
A3	137.2 ± 10.03	117.2 ± 5.09	36.78 ± 0.77
A4	138.3 ± 5.49	118.1 ± 6.31	37.02 ± 1.19

T_m melting temperature; T_c crystallization temperature; ΔH_m melting enthalpy; X_c degree of crystallinity

Fire Behavior

Limiting oxygen indices and combustion characteristics of the samples are given in Table 5. It was observed that the OMMT effectively boosted flame retardancy of HDPE/BF/OMMT nanocomposites with increase in the LOI, and remarkably postponing TTI and decreasing HRR as well as effectively reducing MLR and BR. The nanoclay-produced silicates char on the surface layer of HDPE/BF blends increased the flame resistance of the samples. This was consistent with previous studies [25, 27]. The tortuous path provided by the silicate layers had better barrier property to the oxygen and heat which delayed the burning capacity of the composite [19, 30]. The addition of nanoclay particles increased the thermal degradation temperature and significantly reduced heat release rate and also improved fire retardancy of the nanocomposite. Costache et al. [11] reported that this improvement was due to the high aspect ratio of nanoclay particles, formation of intercalation structure and creation of barrier mechanism. The test results revealed that LOI value of the HDPE, namely oxygen concentration, was significantly increased by the addition of the OMMT (Table 5).

Table 5 Flame data of HDPE/BF/OMMT nanocomposites

Sample code	HRR (kW/m^2)	TTI (s)	MLR (%)	BR (mm/min)	LOI (%)
A_1	68.37 ± 3.19	34.12 ± 1.22	83.17 ± 4.11	46.29 ± 2.16	22.43 ± 0.83
A_2	55.91 ± 2.71	43.08 ± 2.08	78.33 ± 3.52	38.16 ± 1.44	27.58 ± 1.19
A_3	43.24 ± 3.04	52.65 ± 3.11	75.64 ± 1.88	29.73 ± 0.79	31.12 ± 1.05
A_4	37.59 ± 1.84	59.27 ± 2.67	71.31 ± 2.07	24.51 ± 1.03	34.06 ± 0.75

HRR heat release rate; *TTI* time to ignition; *MLR* mass loss rate; *BR* burning rate; *LOI* limiting oxygen index

Mechanical Properties

The effects of OMMT on the tensile strength and modulus of HDPE/BF composites illustrates in Fig. 3. It was observed that incorporation of nanoparticles into polymer matrix increased the both tensile strength and modulus of the composite. Tensile strength and modulus for the samples without OMMT were 27.71 and 3061.44 MPa, respectively. The addition of nanoparticles up to 2 phc loading levels, led to the enhancement of tensile properties, but further increment in the nanoparticles content up to 6 phc loading decreased the tensile strength and modulus. The maximum tensile strength and modulus values were found to be 33.58 and 3361.52 MPa for the composites filled with 2 phc OMMT. This increment in the tensile properties was mainly attributed to the reinforcing effect of OMMT with high aspect ratio [10, 12–16]. It was expected that strong interfacial adhesion between polymer matrix and nanoparticles efficiently transferred the stress and improved the mechanical properties [18–22]. The reduction in the tensile values by further addition of OMMT (from 2 to 6 phc) could be generally explained by the agglomeration or poor dispersion of nanoparticles in polymer matrix [12–16, 18, 20–22]. It could be ascribed to aggregation phenomenon, which caused to the debonding of particles from polymer matrix and/or stress concentration during the mechanical loading.

The flexural strength and modulus of HDPE/BF composites containing different OMMT contents are presented in Fig. 4. There is a clear increasing trend of both flexural strength and modulus with the increase of OMMT content. The flexural properties showed a similar trend to the results of the tensile properties. As shown in Fig. 2, the flexural strength of the control samples without OMMT addition was found to be 18.36 MPa, with a flexural modulus of 1769.84 MPa. The incorporation of 2 phc OMMT led to the increase in the flexural strength and modulus about 37 and 29%, respectively. The significant improvement in the flexural properties was related to the large aspect ratio and high interfacial contact area of the nanoparticles [10, 12–16, 18–22]. As it can be clearly seen from Fig. 4, with an increase in the OMMT content from 2 to 6 phc, the flexural properties decreased. This could be attributed to the poor dispersion due to the tendency of nanoparticles to agglomeration Similar results were reported in previous studies [12–16, 18, 20–22]. For example, Han et al. [14] reported that the addition of clay above a certain point (3 wt%) led to negative effect on mechanical properties of the bamboo composite systems, probably due to migration of clay to the interface between fiber and HDPE.

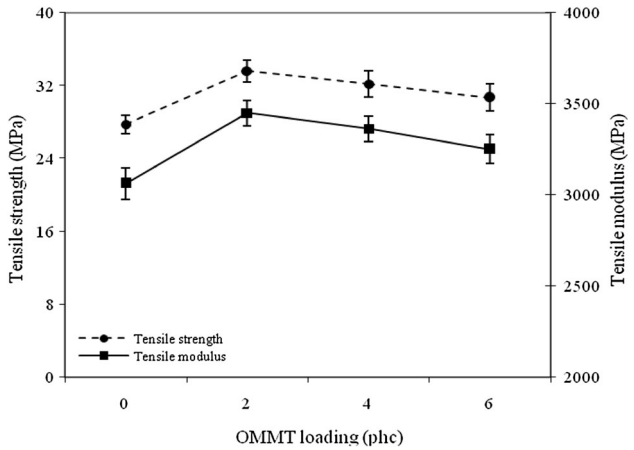

Fig. 3 Tensile strength and modulus of HDPE/BF composites at different loadings of OMMT

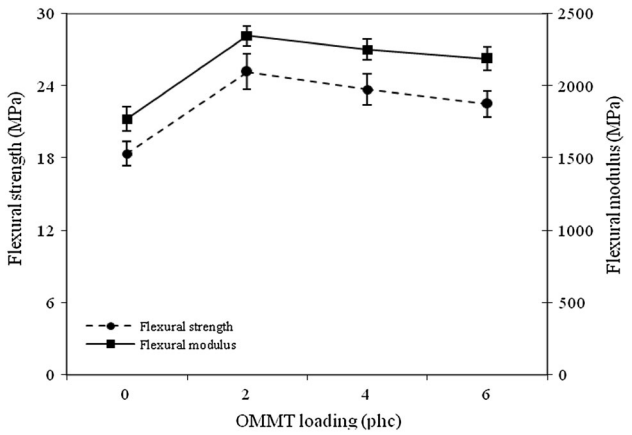

Fig. 4 Flexural strength and modulus of HDPE/BF composites at different loadings of OMMT

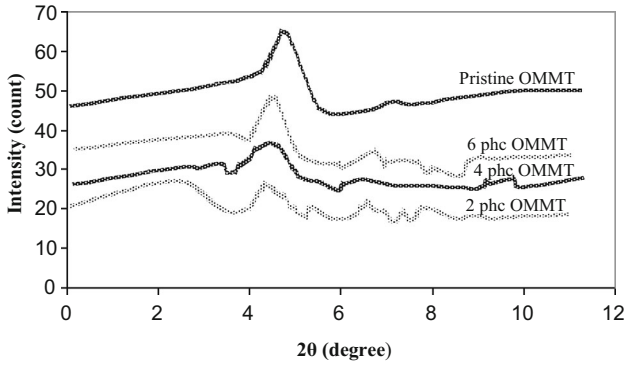

Fig. 5 XRD patterns of HDPE/BF composites with different OMMT content

X-ray Diffraction

The XRD patterns of pure OMMT and HDPE/BF composites with different OMMT content are shown in Fig. 5. As can be seen, the extent of intercalation of samples increased with increase of OMMT content up to 4phc and then decreased. The organically modified nanoclay showed its characteristic intense peak at $2\theta = 4.76°$ with a $d_{001} = 1.85$ nm. In the sample with the addition of 2 phc nanoclay, the peak was shifted to a lower angle ($2\theta = 4.4°$, $d_{001} = 2.006$ nm), which implied the increase in interlayer spacing of silicate layers and intercalation of polymer chains between clay layers. The increase of the interlayer

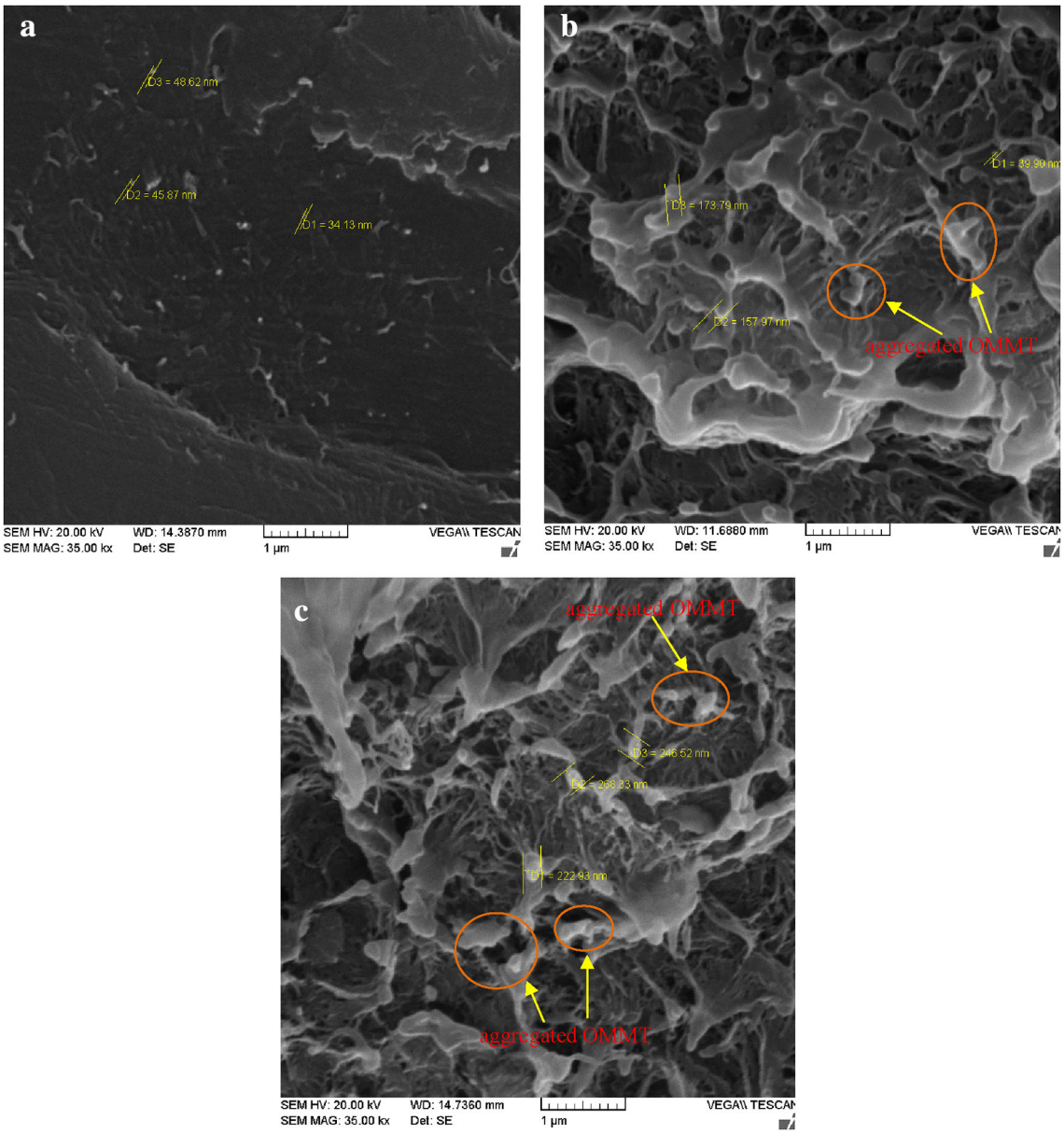

Fig. 6 SEM micrographs of the nanocomposites fractured surfaces: **a** 2 phc OMMT, **b** 3 phc OMMT, **c** 5 phc OMMT

distance might result from the stronger shear during processing when the filler was introduced. The peak of 4 phc nanoclay appeared at $2\theta = 4.48°$, with a $d_{001} = 1.97$ nm. These data show that the order of intercalation for 6 phc nanocaly decreased ($2\theta = 4.54°$, $d_{001} = 1.94$ nm). In fact, by increasing the OMMT loadings, the basal spacing of silicate layers decreased due to the agglomeration of nanoclay particles. In other words, increasing the level of OMMT to 6 phc, the size of dispersed nanoclay became larger or even aggregated in part. Another interesting result in Fig. 5 is that, the nanocaly was not exfoliated, since the peak still obviously existed. Furthermore, formation of an intercalated morphology and better dispersion was shown in 2 phc of OMMT, because the peak of that was shifted to a lower angle.

Morphological Study

The dispersion state of nanoclay in the composites was studied by SEM analysis (Fig. 6). The SEM images clearly showed that well-dispersed nanoparticles resulted in better stress or strain distribution in the composite containing lower OMMT content (Fig. 6a). This dispersion demonstrated that the interfacial adhesion among nanoparticles, fiber, and polymer matrix was markedly improved and further contributed to the stress transfer from fiber to OMMT, which consequently enhanced the performance of the composites. As illustrated in Figs. 6b, c, the size of nanoclay became larger or aggregated with the increase in the level of nanoclay loading up to 6 phc. In other words, the OMMT agglomeration occurred due to its higher loading in the composite. The applied load was distributed unevenly between non-agglomerated and agglomerated OMMT.

Conclusions

In this study, the thermal stability and combustion behavior of HDPE/BF/OMMT nanocomposites by TGA, DSC and CCT techniques were extensively investigated. The data from TGA analysis indicated that the OMMT greatly enhanced the thermal stability. The findings showed that the mechanical properties including tensile and flexural (strength and moduli) increased with increase in the OMMT content up to 2 phc, but then decreased. The maximum tensile strength and modulus values were found to be 33.58 and 3361.52 MPa for the composites filled with 2 phc OMMT. The char residues of the HDPE/BF blends gradually increased with increasing the OMMT content. The highest activation energy was found in the composites containing 6 phc OMMT. The results of DSC behavior of the nanocomposites revealed that the melting temperature (T_m), crystallization temperature (T_c), melting enthalpy (ΔH_m), and crystallinity (X_c) of samples increased. Furthermore, the OMMT was an efficient flame retardant in the composites. The heat release rates, mass loss rate, and burning rate of the nanocomposites decreased in comparison with the HDPE/BF blends. The LOI of the composites considerably increased (22.43–34.06%) as the 6 wt% OMMT was incorporated into the composites. X-ray diffraction patterns indicated that the nanocomposites formed were intercalated, and also the samples containing 2 phc of nanoclay had higher order of intercalation and better dispersion. Based on the findings obtained from the present study, it can be said that the optimum content of the OMMT for the HDPE/BF composites is 2 phc.

References

1. Bledzki AK, Gassan J (1999) Composites reinforced with cellulose based fibers. J Polym Sci 24:221–274
2. Rowell RM, Sandi AR, Gatenholm DF, Jacobson RE (1997) Utilization of natural fibers in plastic composites: problem and opportunities in lignocellulosic composites. J Compos 18:23–51
3. Oksman K, Sain M (2008) Wood-polymer composites. Woodhead Publishing Ltd, Great Abington, p 366
4. Tajvidi M, Takemura M (2009) Effect of fiber content and type, compatibilizer, and heating rate on thermogravimetric properties of natural fiber high density polyethylene composites. Polym Compos 30(9):1226–1233
5. Kim HS, Kim S, Kim HJ, Yang HS (2006) Thermal properties of bio-flour filled polyolefin composites with different compatibilizing agent type and content. Thermochim Acta 451:181–188
6. Yang HS, Wolcott MP, Kim HS, Kim HJ (2005) Thermal properties of lignocellulosic filler-thermoplastic polymer bio-composite. J Therm Anal Calorim 82:157–160
7. Tjong SC (2006) Structural and mechanical properties of polymer nanocomposites: a review. J Mater Sci Eng 53:73–197
8. Viswanathan V, Laha T, Balani K, Agarwal A, Seal S (2006) Challenges and advances in nanocomposite processing techniques: a review. J Mater Sci Eng 54:121–285
9. Utracki LA, Sepehr M, Boccaleri E (2007) Synthetic layered nanoparticles for polymeric nanocomposites (PNCs): a review. J Polym Adv Technol 18:1–37
10. Zhao Y, Wang K, Zhu F, Xue P, Jia M (2006) Properties of poly(vinyl chloride)/wood flour/montmorillonite composites: effects of coupling agents and layered silicate. J Polym Degrad Stabil 91:2874–2883
11. Costache MC, Wang D, Heidecker MJ, Manias E, Wilkie CA (2006) The thermal degradation of poly(methyl methcrylate) nanocomposites with montmorillonite, layered double hydroxides and carbon nanotubes. Polym Adv Technol 17:272–280
12. Wu Q, Lei Y, Clemons CM, Yao F, Xu Y, Lian K (2007) Properties of HDPE/clay/wood nanocomposites. J Plast Technol 27:108–115

13. Lei Y, Wu Q, Clemons CM, Yao F, Xu Y (2007) Influence of nanoclay on properties of HDPE/wood composites. J Appl Polym Sci 18:1425–1433
14. Han G, Lei Y, Wu Q, Kojima Y, Suzuki S (2008) Bamboo–fiber filled high density polyethylene composites; effect of coupling treatment and nanoclay. J Polym Environ 21:1567–1582
15. Hetzer M, Kee D (2008) Wood/polymer/nanoclay composites, environmentally friendly sustainable technology: a review. J Chem Eng 16:1016–1027
16. Ashori A, Nourbakhsh A (2009) Effects of nanoclay as a reinforcement filler on the physical and mechanical properties of wood based composite. Compos Mater 43(18):1869–1875
17. Ghasemi I, Kord B (2009) Long-term water absorption behavior of polypropylene/wood flour/organoclay hybrid nanocomposite. Iran Polym J 18(9):683–691
18. Hemmasi A, Khademieslam H, Talaiepoor M, Ghasemi I, Kord B (2010) Effect of nanoclay on the mechanical and morphological properties of wood polymer nanocomposite. J Reinf Plast Compos 29(7):964–971
19. Kord B (2010) Effect of organomodified layered silicates on flammability performance of HDPE/rice husk flour nanocomposite. J Appl Polym Sci 120:607–610
20. Kord B, Hemmasi A, Ghasemi I (2011) Properties of PP/wood flour/organomodified montmorillonite nanocomposite. Wood Sci Technol 45:111–119
21. Essabir H, Boujmal R, Ouadi BM, Qaiss AK (2016) Mechanical and thermal properties of hybrid composites: oil-palm fiber/clay reinforced high density polyethylene. Mech Mater 98:36–43
22. Ibrahim ID, Jamiru T, Sadiku RE, Kupolati WK, Agwuncha SC (2016) Dependency of the mechanical properties of sisal fiber reinforced recycled polypropylene composites on fiber surface treatment, fiber content and nanoclay. J Polym Environ. doi:10.1007/s10924-016-0823-2
23. Ndiaye D, Tidjani A (2012) Effects of coupling agents on thermal behavior and mechanical properties of wood flour/polypropylene composites. J Compos Mater 46(24):3067–3075
24. Zabihzadeh SM, Ebrahimi GH, Enayati A (2011) Effect of compatibilizer on mechanical, morphological, and thermal properties of chemi-mechanical pulp-reinforced PP composites. J Thermoplast Compos Mater 24:221–231
25. Qin H, Zhang S, Zhao C, Feng M, Yang M, Shu Z, Yang S (2004) Thermal stability and flammability of polypropylene/montmorillonite composites. Polym Degrad Stab 85:807–813
26. Lee SY, Kang IA, Doh GH, Kim WJ, Kim JS, Yoon HG, Wu Q (2008) Thermal, mechanical and morphological properties of polypropylene/clay/wood flour nanocomposites. Exp Polym Lett 2:78–87
27. Guo J, Xu Y, Chen X, Hu S, He M, Qin S (2015) Influences of organic montmorillonite on the combustion behaviors and thermal stability of polyamide 6/polystyrene blends. High Perform Polym 27(4):392–401
28. Biswal M, Mohanty S, Nayak SK (2011) Mechanical, thermal and dynamic-mechanical behavior of banana fiber reinforced polypropylene nanocomposites. Polym Compos 32(8):1190–1201
29. Rajan A, Upadhyaya P, Chand N, Kumar V (2014) Effect of nanoclay on the thermal properties of compatibilized ethylene vinyl acetate copolymer/high-density polyethylene blends. J Thermoplast Compos Mater 27(5):650–662
30. Devi RR, Gogoi K, Konwar BK, Maji TK (2013) Synergistic effect of nano TiO_2 and nanoclay on mechanical, flame retardancy, UV stability, and antibacterial properties of wood polymer composites. Polym Bull 70:1397–1413
31. Ayrilmis N, Kaymakci A, Ozdemir F (2013) Physical, mechanical, and thermal properties of polypropylene composites filled with walnut shell flour. J Ind Eng Chem 19:908–914